RSC Advances

This is an *Accepted Manuscript*, which has been through the Royal Society of Chemistry peer review process and has been accepted for publication.

Accepted Manuscripts are published online shortly after acceptance, before technical editing, formatting and proof reading. Using this free service, authors can make their results available to the community, in citable form, before we publish the edited article. This *Accepted Manuscript* will be replaced by the edited, formatted and paginated article as soon as this is available.

You can find more information about *Accepted Manuscripts* in the Information for Authors.

Please note that technical editing may introduce minor changes to the text and/or graphics, which may alter content. The journal's standard Terms & Conditions and the Ethical guidelines still apply. In no event shall the Royal Society of Chemistry be held responsible for any errors or omissions in this *Accepted Manuscript* or any consequences arising from the use of any information it contains.

ROYAL SOCIETY OF CHEMISTRY

www.rsc.org/advances

Enhanced reverse saturable absorption of electrostatic self-assembled layer by layer films containing (8-quinolineoxy-5-sulfonic acid) phthalocyanine cobalt and graphene oxide

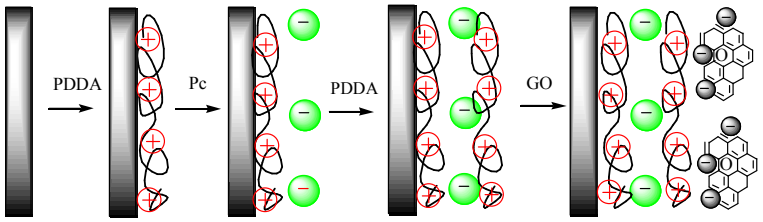

The 25-bilayer CoPc/GO film was fabricated through electrostatic self-assembled layer by layer (LBL) technique, and it exhibits strong reverse saturable absorption (RSA) effect with the input intensity of 1.16 μJ.

RSC Advances Accepted Manuscript

Enhanced reverse saturable absorption of electrostatic self-assembled layer by layer films containing (8-quinolineoxy-5-sulfonic acid) phthalocyanine cobalt and graphene oxide

Bowen Chen,[a] Chunying He,*[a] Weina Song,[ab] Cheng Zhao,[a] Yachen Gao,[a] Zhimin Chen,[a] Yongli Dong,[ab] Yiqun Wu[a] and Rong Li[a]

[a] *Key Laboratory of Functional Inorganic Material Chemistry, Ministry of Education, School of Chemistry and Materials Science, Heilongjiang University, Harbin 150080, PR China*

[b] *College of Environmental and Chemical Engineering, Heilongjiang University of Science and Technology, Harbin 150022, PR China*

Abstract

Multilayer films containing α-CoPc($QnSO_3Na$)$_4$ (CoPc), polydiallydimethyldially-lammonium chloride (PDDA) and graphene oxide (GO) were fabricated through electrostatic self-assembled layer by layer (LBL) technique. UV-Vis spectroscopy was used to characterize the assembly process. Raman spectroscopy, scanning electron microscopy (SEM) and atomic force microscopy (AFM) were utilized to explore the microstructure of the film. The third-order nonlinear properties of the film were studied by Z-scan measurements at 532 nm with 4 ns pulses. When excited by laser with the input intensity of 1.16 μJ, the 25 bilayer CoPc/GO film exhibits strong reverse saturable absorption (RSA) effect. The nonlinear absorption coefficient β value is 1.6×10^{-5} m/W, which is 5 and 3 orders larger than that of CoPc solution sample and grapheme oxide solution sample, and 1.5 times larger than that of the 35 bilayer CoPc/PDDA film. And also, combination of UV-Vis spectroscopy with Raman spectroscopy was adopted to analyze the enhancement mechanism of nonlinear optical absorption of the film.

Introduction

The development of photonic and optoelectronic technologies relies on the new

* Corresponding author: Fax: +86 451 8667 3647

E-mail address: chunyinghe_hlju@163.com (C. He)

RSC Advances Accepted Manuscript

nonlinear optical (NLO) materials including inorganic crystals, metal clusters, polymers, C_{60}, phthalocyanines, etc.[1-5] Past research shows that materials with π conjugated system often exhibit strong third-order NLO properties, which can be used as candidates in optical switching devices. Optical switching is a fundamental building block of information processing, and has been reported in various materials, such as phthalocyanines[6,7] and graphene oxide[8,9]. In recent years, graphene-based materials show great promise in ultrafast lasers as saturable absorbers due to their ultrafast carrier relaxation times and broadband NLO responses to nanosecond pulses from the visible to the near-infrared regime.[10-12] GO has covalently bounded epoxide and hydroxyl functional groups on either side of its basal plane with carboxyl groups only at the edge sites. These hydrophilic groups make GO easily to connect with other functional materials, such as nanoparticles, porphyrins, and pthalocyanines.[13-16] GO sheets contain a mixture of electronically conducting sp^2 clusters, sp^2 configurations and insulating sp^3 carbon matrix,[17,18] which make GO displaying excellent third-order NLO properties under nanosecond, picosecond, and femosecond laser excitation at the wavelength of 532 nm and 1064 nm.[19-21] Calculations based on Gaussian and time-dependent (TD) density functional theory (DFT) about the band gaps of sp^2 cluster and sp^3 carbon matrix in GO sheets are around 0.5 eV and 2.7-3.1 eV, respectively, resulting in saturable absorption (SA) effect and excited state absorption (ESA) effect.[19-20,22] Composite materials based on GO have been fabricated, and their third-order NLO properties were tuned by controlling the ratio of sp^2/sp^3 carbons.[23-25]

Because of the significant π-electron conjugation, high architectural flexibility and fast NLO response times, phthalocyanines and their derivatives have emerged as the important class of materials for NLO applications.[26,27] Naturally, it became one kind of the most important materials which could attach to GO and affect the NLO properties of GO. Indeed, it is expected that the combination of graphene and active phthalocyanine molecules would afford species that possess not only the intrinsic properties of phthalocyanine and GO, but also multifunctional materials with enhanced the third-order NLO responses compared with that of the individual graphene and phthalocyanine. Some hybrids based on both graphene and

RSC Advances Accepted Manuscript

phthalocyanines with excellent NLO properties have been reported.[28,29] However, above NLO performance of GO and its composite materials has been most investigated in the liquid form. Endeavors make great efforts to fabricate the excellent homogeneously disperse GO solid materials.[30,31] Previous studies manifest that the ultrathin film with highly ordered molecular assemblies usually generates a larger NLO effect, including the electrostatic layer by layer (LBL) films.[32,33] Recently, many researchers devote to the fabrication of the film mentioned above to explore the optical nonlinear materials with potential advantage in device application. To the best of our knowledge, the composite films containing phthalocyanine and GO with excellent third-order NLO properties which were prepared using the electrostatic layer by layer (LBL) technique have never been reported.

In this paper, the fabrication and characterization of nanostructure multilayer films, named as CoPc/PDDA/GO (CoPc/GO) film, consisting of anionic CoPc, GO and PDDA through electrostatic LBL self-assembly technique was reported. And also the CoPc/PDDA film and the GO/PDDA film were prepared. The third-order NLO properties of these films and the corresponding solution samples were investigated using the Z-scan technique.[34] The CoPc/GO film displayed stronger RSA effect with larger nonlinear absorption coefficient in comparison with its corresponding film and aqueous sample. The enhanced NLO mechanism for the CoPc/GO film was investigated. In earlier experiments, the third-order optical nonlinearities of the 26 bilayer CuPc$(COONa)_4$/PDDA film with 4 ns width was studied by our group.[35] The nonlinear absorption coefficient β value of the 25 bilayer CoPc/PDDA is two times as large as that of the 26 bilayer CuPc$(COONa)_4$/PDDA film.

Materials

1,8,15,22-tetrakis (8-quinolineoxy-5-sulfonic acid) phthalocyanine cobalt [CoPc] (Fig. 1) was synthesized from 3-(5-sulfonic quinoline-8-oxy) phthalonitrile. The synthetic route of 3-(5-sulfonic quinoline-8-oxy) phthalonitrile is similar to that in reference.[36] 3-(5-sulfonic quinoline-8-oxy) phthalonitrile (0.4 mmol), $CoCl_2$ (0.1 mmol), 1-hexanol (15 ml) and 1,8-diazabicyclo [5.4.0] undec-7-ene (DBU) (0.7 ml)

RSC Advances Accepted Manuscript

were mixed together. The mixture was stirred and refluxed for 24 h under a nitrogen atmosphere. After cooling to room temperature, the organic solvent was removed through vacuum distillation. The obtained product was purified by column chromatography (silica gel, MeOH). The green eluant was collected and was concentrated to 2 ml via rotary evaporation method. And then a mount of CH_2Cl_2 was added into the concentrated solution to the solid product precipitated, and it was filtered off. Yield: 0.21 g (67%). IR [(KBr) ν_{max} (cm^{-1})]: 3423 (S–O–H), 3093 (Ar–H), 1633, 1598 (C＝N, C＝C), 1195 (Ar–O–Ar), 1128 (O–S–O), 1041 (C–S). UV-Vis (DMSO): λ_{max} = 674 (4.51×10^4), 292 (2.49×10^4). MALDI-TOF-MS Found (Calcd): 1464.3 (1464.3).

Preparation of the layer by layer films

The tetrasodium salts of CoPc and GO were obtained through the reaction of CoPc and GO with sodium hydroxide solution, respectively, and the concentrations of CoPc water solution and GO were 1 mg/mL, and 0.1 mg/mL, respectively. PDDA (MW ca. 100,000-200,000 Aldrich）solution and anionic sodium poly(styrenesulfonate) (PSS, MW 70, 000, Aldrich) solution for the preparation of composite film were diluted to 10 wt% aqueous solution. The molecular structures applied to the preparation of the mutilayer films are shown in Fig. 1. Three layers of PDDA/PSS were firstly deposited on the surface of the pre-treated substrates.[32,33] And then the substrate was dipped into the CoPc, PDDA and GO aqueous solution alternately. Once the dipping ends, the substrate was cleaned with deionized water and dried with a stream of nitrogen gas. The recycling fashion was repeated until the desired number of bilayers was obtained. The electrostatic layer by layer films of CoPc/PDDA, and GO/PDDA film were also prepared according to above method. The buildup process of the multilayer films is described as Fig. 2.

Measurements

The film thickness was performed on the step profiler (Taylar Hobson PGI 1240). The multilayer growth process was monitored with Perkin-Elmer Lambda

RSC Advances Accepted Manuscript

900UV/Vis/NIR spectrometer. The total thickness of the 25 bilayer CoPc/GO film and the 35 bilayer CoPc/PDDA film are 243.7 nm and 247.3 nm, respectively, obtained through the step profiler (Dektak150). Atomic force microscopic (AFM) images were taken in air at room temperature with nanoscopic Ⅲ instrument (digital instrument) operating in tapping mode. Raman spectra were performed at room temperature with HR800 spertrometer (λ=458 nm). The scattered light is collected by the same objective in back scattering configuration and detected by a charge-coupled device (CCD). Scanning electron microscope (SEM) micrographs were aquaired using a HELIOS NANOLAB 600i instrument (FEI company). The third-order nonlinear optical properties were investigated using the Z-scan technique with a Q-switching Nd:YAG laser system which produced 4 ns laser pulses at 532 nm at a 1 Hz repetition rate. The spatial and temporal distribution of the pulses was nearly a Gaussian profile. The focal length of the converging lens used in the experimental setup is 10 cm.

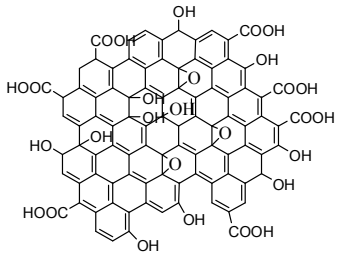

GO

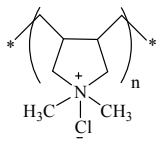

PDDA

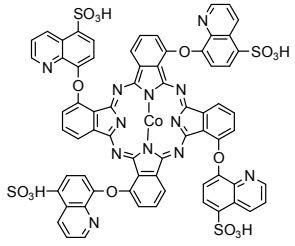

CoPc

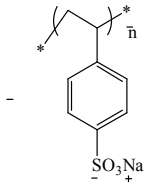

PSS

Fig. 1 The molecular structures of GO, CoPc, PDDA and PSS

RSC Advances Accepted Manuscript

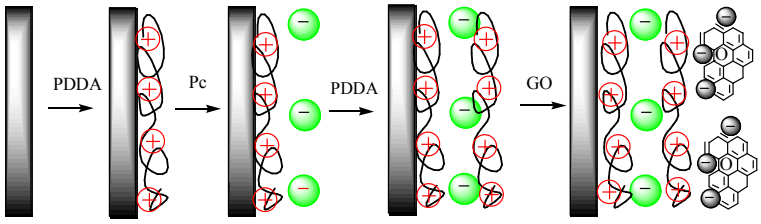

Fig. 2 Procedure for fabrication of CoPc/GO film by alternating deposition.

RESULTS AND DISCUSSION

UV-Vis spectra

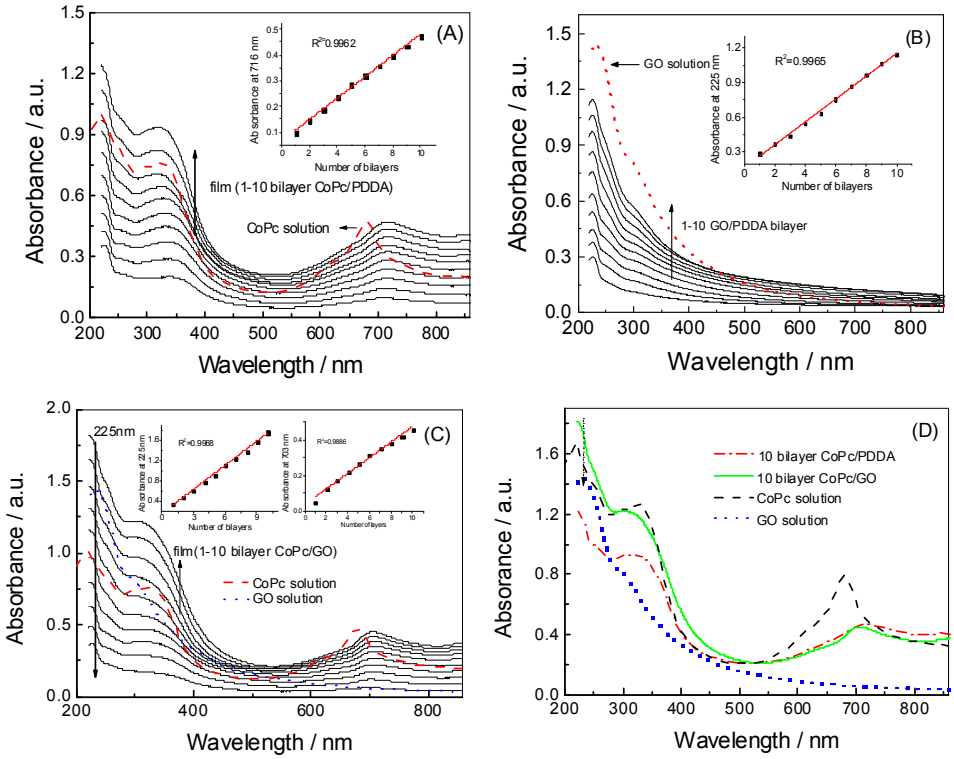

Fig. 3 UV-Vis absorption spectra of films and solution samples. (A) 1-10 bilayer CoPc/PDDA films, and CoPc aqueous solution. Inset shows the relationship of the absorbance in Q band and the number of bilayers. (B) 1-10 bilayer GO/PDDA films and GO aqueous solution. (C) 1-10 bilayer CoPc/GO multilayer films, GO aqueous solution and CoPc aqueous solution. The right inset shows the relationship of the Q band absorbance of the film at 703 nm and the number of bilayer, and the left inset plot implies the absorbance of the film at 225 nm versus the number of bilayers. (D) The 10 bilayer CoPc/PDDA film, the 10 bilayer CoPc/GO film, CoPc aqueous solution, and GO aqueous solution.

Fig. 3(A) shows the UV-Vis spectra of CoPc aqueous solution and the film from 1-10 bilayer every other five bilayers deposited on the quartz substrate. The Q bands

RSC Advances Accepted Manuscript

of CoPc exist whether in UV-Vis spectra of the film or that of aqueous solution. The absorption maximum for Q-band of the film is red-shifted by 36 nm relative to the aqueous solution of CoPc, suggesting that face to face aggregation occurred in the film.[37] The same amount of CoPc molecules deposited on the surface of the substrate, which can be deduced from that the absorbance at both the Soret-band and Q-band increases linearly with the number of layers. The insert plot implies the absorbance of the film at 716 nm versus the number of bilayers, indicating a stepwise and regular process.

The UV-Vis spectra of 1-10 bilayer GO films and aqueous solution are shown in Fig. 3(B). The larger linear regression value of 0.9965 in the insert plot at 225 nm shows that the average amount of GO was deposited on the substrate.

The UV-Vis spectra of CoPc aqueous solution, GO aqueous solution and the film of CoPc/GO from 1-10 bilayer are shown in Fig. 3(C). The right insert shows the linear relationship between the film layers and absorbance of the film at 703 nm. The degree of linear regression was 0.9886, according to the Lambert-Beer law, the same amount of CoPc molecules are deposited in every bilayer. From Fig. 3(C), the information about absorption peak of the GO solution at 225 nm could also be obtained, and the left insert of Fig. 3(C) shows the relationship between absorbance of the CoPc/GO film at 225 nm and the number of bilayers. The linear fit yields linear regression (R^2=0.9968), indicating that the adsorption of GO sheets on the surface of the substrate was regular in every cycle.

Fig. 3(D) shows the UV-Vis spectra of the 10 bilayer CoPc/PDDA film and 10 bilayer CoPc/GO film. The spectrum of CoPc/GO film exhibits the characteristic Q and S bands of phthalocyanine complex, indicating that Pc molecules deposited on the surface of the substrate. Both the absorbance of the two kinds of the films is almost the same, showing that the two kinds of films contained the same amount of Pc molecules. The absorbance of the 10 bilayer CoPc/GO film is much stronger than that of the 10 bilayer CoPc/PDDA film in the range of 200-400 nm on account of the deposition of GO sheets on the surface of the substrates in every alternate cycle. Compared with the spectra of GO aqueous solution, the absorption peak of the 10

RSC Advances Accepted Manuscript

bilayer CoPc/GO film within the S band is blue shifted with 6 nm because the relocation of the electron from the graphitic clusters of GO to Pc happened.[16] The absorbance of 35 bilayer CoPc/PDDA at 225 nm is about 4.2, and the absorbance of 25 bilayer CoPc/GO at 225 nm is about 5.0, both of them exceed measuring range of UV-vis spectrometer.

Morphological analysis

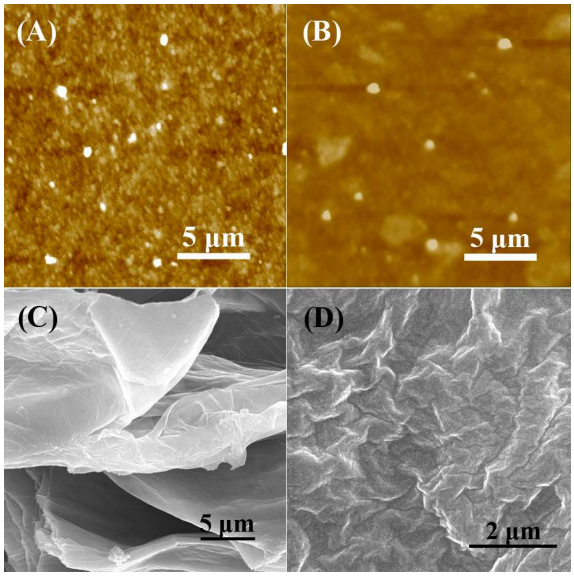

Fig. 4 AFM images of the 35 bilayer CoPc/PDDA film (A) and the 25-bilayer CoPc/GO film (B). SEM images of GO powder (C) and the 25 bilayer CoPc/GO film (D).

The tapping mode AFM image of the 35 bialyer CoPc/PDDA films doposited on the silicon wafer is shown in Fig. 4(A). The surface of the substrate was covered by dense packing circular nanoparticles with an average diameter of about 12.74 nm, and the mean interface roughness is 12.837 nm. However, the AFM images of CoPc/GO are very different from that of the CoPc/PDDA films. Fig. 4(B) shows the tapping mode AFM image of the 25-bilayer CoPc/GO film deposited on the silicon wafer, verifying dense coverage of platelets with the average diameter of 3.38 μm which is very larger than the average size of GO sheet (about 0.5-1 μm) and one Pc molecule (0.7 nm^2).[38,39] Therefore, GO sheets and Pc molecules aggregate to each other in the composite films. It reveals that the surface of the film is rather flat, and the mean interface roughness is 2.649 nm. It can be easily seen from Fig. 4(B) that GO platelets become orientated parallel to the surface of the substrate, and present the irregular

RSC Advances Accepted Manuscript

edges. The SEM image (Fig. 4(C)) of GO powder shows the multilayer flake structure. The SEM image of the 25 bilayer CoPc/GO film reveals the smooth surface of the LBL film with tiny wrinkles (Fig. 4(D)), which are caused by the compositional and topographic of the nanosheets. Above results indicate that the graphene nanosheets and phthalocyanines aggregate in the composite film.

Raman spectra

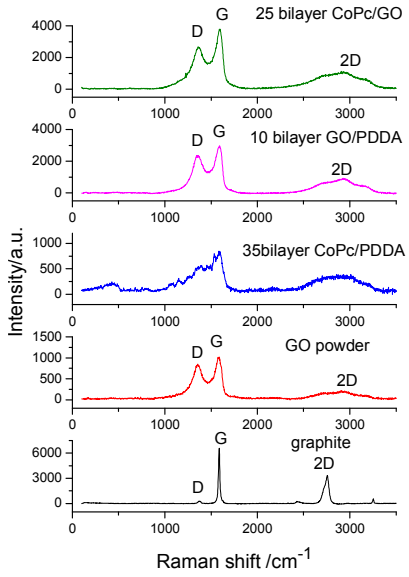

Fig. 5 Raman spectra of the 25 bilayer CoPc/GO film, the 10 bilayer GO/PDDA film, the 35 bilayer CoPc/PDDA film, GO powder and graphite powder

Raman spectroscopy has been utilized as a powerful tool for the characterization of graphene-based materials, as it can be used to identify the number of layers, the edge of structure, the type of doping, and any defects in graphene-based materials. As for graphene oxide, it is actually consists of two parts, that is graphite cluster and oxygen functional groups. The G band represents sp^2 carbon atoms domains, arising from the first-order scattering of E_{2g} phonons from sp^2 carbon atoms. D band is generally related to the vibrations of sp^3 carbon atoms, corresponding to the mode of κ-point phonons of A_{1g} symmetry. CoPc have almost 10 vibrations in Raman spectra, among which only the fingerprint bands are described in this report. The most intense Raman bands are found at 432.3, 1154.0, 1394.6, 1590.3 cm^{-1}. The Raman spectra of

RSC Advances Accepted Manuscript

graphite display a strong G band at 1586.2 cm^{-1}, and a very weak D band at 1370.1 cm^{-1}. Instead, obvious stronger and broader D band compared to the graphite was observed for the GO powder, the 10 bilayer CoPc/PDDA and the 25 bilayer CoPc/GO. This can be attributed to the presence of the oxygen functional groups induced defects during the preparation of graphene oxide.[40] While, the D band and G band of the 10 bilayer GO/PDDA films are at 1366 and 1598 cm^{-1}. The 25 bilayer CoPc/GO film displays two prominent peaks at 1361 and 1596 cm^{-1} corresponding to the D band and G band. The G band of the 25 bilayer CoPc/GO film is red shifted by 4 cm^{-1} compared to that of GO powder (1592 cm^{-1}). Through the π-π interaction between the graphene domain of GO and phthalocyanine, the relocation of electron from the GO to Pc happened,[41] which was also verified by the blue shift of the absorption peak with 6 nm compared to that of GO aqueous solution in Fig. 3(D).[16] The I_D/I_G ratio was 0.70, which was smaller than that of 10 bilayer GO/PDDA films (0.79), and GO powder (0.83). The reason may be that CoPc molecules grafted onto GO sheets contain a large amount of sp^2 aromatic carbon atoms, and furthermore the G band of CoPc/GO was enhanced, indicating the successful adsorption of Pc and GO to the films.

Third-order NLO measurements

The Z-scan technique is adopted to study the third-order NLO properties of the 25 bilayer CoPc/GO film. In order to investigate the nonlinear mechanism of the 25 bilayer CoPc/GO film, the same experiments were conducted with the 25 bilayer CoPc/PDDA film on account of both the two kinds of films containing the same amount of phthalocyanines (Fig. 3(D)). Since the absorbance of the 10 bilayer GO/PDDA film and the 10 bilayer CoPc/PDDA film at 225 nm are 1.146 and 1.23, respectively, while the absorbance of the 25 bilayer CoPc/GO film is 1.75 at 225 nm from Fig. 3(D). Certainly, the amount of GO in the 25 bilayer CoPc/GO film is not more than that in the 10 bilayer GO film. Therefore, the Z-scan nonlinear experiments on the 10 bilayer GO film under the same conditions were also carried out. The absorbance of 0.13 mg/mL GO aqueous solution at the maximum absorption

RSC Advances Accepted Manuscript

wavelength of 225 nm is 2.53, which is much stronger than that of the 10 bilayer GO film. And, the absorbance of 0.13 mg/mL CoPc aqueous solution at the maximum absorption wavelength of 680 nm is 2.258, while the absorbance of 25 bilayer CoPc/GO at 704 nm is about 1.35. So, the third-order NLO properties of 0.13 mg/mL CoPc and 0.13 mg/mL GO aqueous solution sample were performed under the identical experimental conditions except the incident energy.

Fig. 6 (A)-(C) show the open-aperture Z-scan curves of the 25-bilayer CoPc/GO film on the quartz substrate at the linear transmittance of 28.0 %, the 35 bilayer CoPc/PDDA film on the quartz substrate at the linear transmittance of 74.0 %, CoPc aqueous solutions at the linear transmittance of 75.0 % in the quartz cell and GO aqueous solutions at the linear transmittance of 42.0 % in the quartz cell. The valleys of the normalized transmittances indicate that above three samples behave reverse saturable absorption (RSA) effect. But, nonlinear absorption of the sample transformed from SA to RSA as the sample approached focal point for the normalized transmittance of GO solution sample. These samples did not display any nonlinear refraction effect. The following equations were used to fit above results. In Z-scan measurement systems, the input laser beam can be considered as TEM_{00} Guassian beam as given as:[34]

$$I_i = \frac{I_0 \exp\left[-2\left(r/\omega\right)^2 - \left(t/t_0\right)^2\right]}{1+\left(z/z_0\right)^2} \tag{1}$$

Where, $z_0 = \pi\omega_0^2/\lambda$, ω_0 is the beam waist (50 μm in this measurement system), r is the distance from the axis of the beam, and ω is the radius of the beam at the z-position. The exit laser intensity from the sample may be obtained as:

$$I_t = I_i(r,t,z)e^{-\alpha L} \tag{2}$$

where L is the thickness of the sample, z is the sample position and α is the absorption coefficient.

In the determination of the nonlinear absorption coefficient β of the samples

RSC Advances Accepted Manuscript

taking into account the observed bleaching of the sample transmission occurring at lower pump intensity region, the corresponding Z-scan recordings were fitted by using the intensity variation equation and adopting an intensity-dependent absorption coefficient. The absorption coefficient α had the form $\alpha = \alpha_0/(1 + I/I_s) + \beta I$, where α_0 is the linear absorption coefficient, I_s is the saturation intensity, β is the nonlinear absorption coefficient and I is the laser intensity within the sample.

The theoretical fits to the Z-scan data were calculated from the normalized transmittance equation:

$$T(z,S) = \frac{\int_{-\infty}^{\infty} P_o(t)dt}{\int_{-\infty}^{\infty} P_i(t)dt} \quad (3)$$

Where, $P_i(t) = (\pi\omega_0^2/2)I_0\exp[-(t/t_0)^2]$ is the instantaneous input power, $P_o(t) = (\pi\omega_0^2/2)I_t\exp[-(t/t_0)^2]$ is the output power. The fitting nonlinear absorption coefficients of the film samples and solution samples are listed in Table 1, and above coefficients obtained under the other input intensities of laser for each sample are also listed in Table 1.

From Table 1, the nonlinear absorption coefficient β value of CoPc aqueous solution sample is positive, illustrating that the curve of CoPc solution displays a typical valley of RSA behavior, corresponding to the absorption of the triplet excited state. When the laser energy reached the 62.8 μJ, CoPc solution sample displayed SA effect. This is because most of phthalocyanine molecules were excited to the first triplet excited state and high order nonlinear optical absorption happened. Owing to the better solubility of CoPc molecules in alkaline aqueous solution and small volume of CoPc molecules, any scattering phenomenon was not observed.

RSC Advances Accepted Manuscript

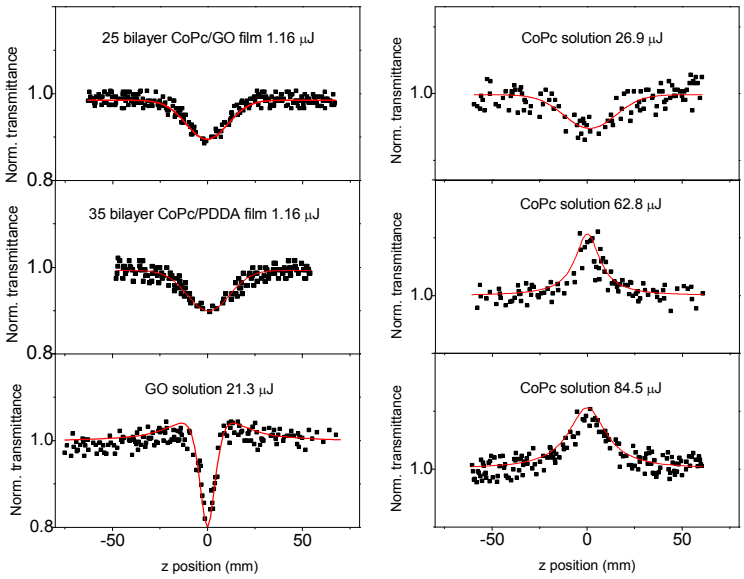

Fig. 6 The open-aperture normalized Z-scan transmittance curves of the 25-bilayer CoPc/GO film, the 35 bilayer CoPc/PDDA film, CoPc aqueous solution and GO aqueous solution

From Fig. 6, the normalized transmittance curve of GO aqueous solution sample exhibits two shoulder peaks along with a valley corresponding to a transformation from SA to RSA as the sample approach focal point. The nonlinear absorption coefficient β values of GO decrease from 5.0×10^{-9} m/W to 2.3×10^{-9} m/W when the input intensity increases from 21.3 μJ to 62.8 μJ (Table 1). A comprehensive analysis on the β value and the normalized nonlinear absorption curves of GO reveals that the optical nonlinearities of GO alkaline aqueous solution are mainly from nonlinear absorption and weaker nonlinear scattering.[42] After excited by lower laser intensity, the SA effect originating from Pauli blocking dominates the NLO absorption on account of the state filling of the interband transitions in the sp^2 clusters. On the other hand, the two photo absorption (TPA) originating from the sp^3 domains dominates the NLO absorption due to high energy gap of sp^3-bonded carbon (2.7-3.1 eV) and sp^2 configurations at relative high input intensities.[21,43] In general case, TPA will happen if transformation from SA to RSA as the sample approach focal point is observed.[44] The nonlinear scattering should exist on account of the large volume of GO sheet relative to the phthalocyanine molecules. However, the nonlinear scattering effect is secondary in comparison to the nonlinear absorption because the influence of nonlinear scattering will be enhanced at relative high input intensities. The larger the

RSC Advances Accepted Manuscript

input intensity is, the stronger the scattering effect is. When the solution sample was excited by nanosecond laser, the thermal effect should exist. In the experiments, the thermal effect is not considered because it affects only nonlinear refraction, not nonlinear absorption.

Table 1 The third-order NLO parameters of the 25-bilayer CoPc/GO film, the 35-bilayer CoPc/PDDA film, CoPc aqueous solution and GO aqueous solution

Samples	$E(\mu J)$	T_0	β (m/W)	Concentration or number of bilayer
Film(CoPc/GO)	1.16	28.0	1.6×10^{-5}	25 bilayer
Film(CoPc/GO)	1.56	20.0	-1.3×10^{-5}	25 bilayer
Film(CoPc/GO)	2.26	18.0	-9.5×10^{-6}	25 bilayer
Film(CoPc/PDDA)	1.16	74.0	1.0×10^{-5}	35 bilayer
Film(CoPc/PDDA)	1.56	74.0	9.0×10^{-6}	35 bilayer
Film(CoPc/PDDA)	2.26	74.0	4.0×10^{-6}	35 bilayer
Solution(CoPc)	26.9	75.0	5.3×10^{-11}	0.13mg/mL
Solution(CoPc)	40.2	75.0	4.9×10^{-11}	0.13mg/mL
Solution(CoPc)	62.8	75.0	-4.6×10^{-11}	0.13mg/mL
Solution(CoPc)	84.5	75.0	-3.4×10^{-11}	0.13mg/mL
Solution(GO)	21.3	42.0	5.0×10^{-9}	0.13mg/mL
Solution(GO)	40.2	42.0	4.5×10^{-9}	0.13mg/mL
Solution(GO)	62.8	42.0	2.3×10^{-9}	0.13mg/mL
Solution(GO)	84.5	42.0	2.3×10^{-9}	0.13mg/mL

Since PDDA and PSS did not display any third-order NLO effect in our experiment, it is reasonable for us to deem that the RSA effect of the 25 CoPc/GO film results from CoPc molecules and GO sheets, and CoPc is the only source of nonlinear absorption effect for the CoPc/PDDA film. The 25 bilayer CoPc/PDDA film and the 10 bilayer GO/PDDA film did not show any third-order NLO properties under the same experimental conditions. However, the 25 bilayer CoPc/GO film exhibits

RSC Advances Accepted Manuscript

strong RSA effect, with the nonlinear absorption coefficient β value of 1.6×10^{-5} m/W, which is 5 and 3 orders larger than that of the CoPc solution sample and GO solution sample, and 1.5 times larger than that of the 35 bilayer CoPc/PDDA film (Table 1).

But, it is interesting that SA effect disappeared in the 25 bilayer CoPc/GO film. As for the CoPc/GO film, the resource of nonlinear absorption results from the π conjugated macrocycle systems of phthalocyanine, the sp^3 domains and sp^2 configurations in GO sheets. The π conjugated macrocycle systems of phthalocyanine and sp^2 configurations in GO sheets are related to the absorption of the triplet excited state, and sp^3 domains dominate the NLO absorption due to the high energy gap of sp^3 bonded carbon (2.7-3.1 eV). The stronger nonlinear absorption effect of the 25 bilayer CoPc/GO film with contrast to the corresponding film and solution is explained in detail as follows. The graphitic domain is mainly composed of sp^2 carbon, which apt to interact with the Pc ring through the π-stacking mechanism, thus producing the larger π conjugated system. Furthermore, the relocation of the electron from the GO sheets to Pc happened between the graphitic cluster of GO and phthalocyanine which was verified by the results of Raman (Fig. 5) and UV-Vis experiments (Fig. 3(D)). So, the SA effect was not been observed from the normalized transmittance of CoPc/GO film, and the RSA effect from the phthalocyanines and sp^3 matrix in GO sheets was enhanced. Excited by the laser with the input intensity of 1.56 μJ, the SA effect of the 25 bilayer CoPc/GO film can be ascribed to the formation of more and larger sp^2 clusters upon laser-induced reduction.[21] Correlative evidence is also obtained by comparing the β value of the 35 bilayer CoPc/PDDA film with that of the 25 bilayer CoPc/GO at the input intensity of 1.56 μJ and 2.26 μJ. It is noticed that the β value of the 35 bilayer CoPc/PDDA film is decreases from 1.0×10^{-5} m/W to 4.0×10^{-6} m/W with the increasing input intensity, but it is still positive. This is because there is no any sp^3-hybridized carbon matrix which could be reduced.

Conclusion

In conclusion, we have fabricated multilayer films containing CoPc, PDDA and graphene oxide (GO) using electrostatic self-assembled layer by layer (LBL) technique. The platelet-like flat structure with wrinkles was observed on the surface

RSC Advances Accepted Manuscript

of the substrate. The 25 bilayer CoPc/GO film exhibits strong RSA effect in comparison with the corresponding film and solution samples. The reason why the SA effect of GO solution disappeared at lower pump intensities and RSA enhancement of CoPc/GO film compared to the corresponding film and solution was presumed that sp^2 cluster of GO sheets interact with the Pc ring through the π-stacking, thus producing the larger π conjugated system; the relocation of the electron from the GO sheets to Pc happened between the graphitic cluster of GO and phthalocyanine which was verified by the results of Raman and UV-Vis experiments. The CoPc/GO film is the promising material used in the fast optical switching devices.

Acknowledgments

This work is supported by the National Natural Science Foundation of China (21203058, 51002046 and 61275117), Natural Science Foundation of Heilongjiang Province of China (B201308, F201112), Foundation of Educational Commission of Heilongjiang Province of China (12521399 and 12531579), Natural Science Foundation for the Returned Overseas Scholars of Heilongjiang Province (LC2012C02) and the Innovative Talents Program of Heilongjiang University of Science and Technology (Q20130202).

Reference

1 T. L. Chen, Z. H. Sun, J.-P. Niu, Q.-G. Zhai, C. G. Jin, S. Y. Wang, L. N. Li, Y. Wang, J. H. Luo and M. C. Hong, *J. Cryst. Growth*, 2011, **325**, 55-59.

2 K. Zhou, C. Qin, L.-K. Yan, W. E. Li, X.-L. Wang, H.-N. Wang, K.-Z. Shao and Z.-M. Su, *Dyes and Pigments*, 2015, **113**, 299-306.

3 A.-L. Roy, C. Bui, I. Rau, F. Kajzar, B. Charleux, M. Save, D. Kreher and A.-J. Attias, *Polymer*, 2014, **55**, 782-787.

4 M. D. Zidan, A. W. Allaf, A. Allahham and A. AL-Zier, *Opt. Laser Technol*., 2015, **68**, 60-66.

5 K. E. Sekhosana, E. Amuhaya and T. Nyokong, *Polyhedron*, 2015, **85**, 347-354.

RSC Advances Accepted Manuscript

6 F. Z. Henari, *J. Opt. A: Pure Appl. Opt.*, 2001, **3**, 188-190.

7 C.-B. Yao, Y.-D. Zhang, D.-T. Chen, H.-T. Yin, C.-Q. Yu, J. Li and P. Yuan, *Opt. Laser Technol.*, 2013, **47**, 228-231.

8 S. Roy and C. Yadav, *Appl. Phys. Lett.*, 2013, **103**, 241113.

9 P. Joo, B. J. Kim, E. K. Jeon, J. H. Cho and B.-S. Kim, *Chem. Commun.*, 2012, **48**, 10978–10980.

10 G. K. Lim, Z. L. Chen, J. Clark, R. G. S. Goh, W. H. Ng, H. W. Tan, R. H. Friend, P. K. H. Ho and L. L. Chua, *Nat. Photonics*, 2011, **5**, 554-560.

11 J. Wang, Y. Hernandez, M. Lotya, J. N. Coleman and W. J. Blau, *Adv. Mater.*, 2009, **21**, 2430-2435.

12 M. Feng, H. B. Zhan and Y. Chen, *Appl. Phys. Lett.*, 2010, **96**, 033107.

13 V. Etacheri, J. E. Yourey and B. M. Bartlett, *ACS Nano*, 2014, **8**, 1491-1499.

14 M. K. Kavitha, H. John, P. Gopinath and R. Philip, *J. Mater. Chem. C*, 2013, **1**, 3669-3676.

15 D. K. Huang, J. F. Lu, S. H. Li, Y. P. Luo, C. Zhao, B. Hu, M. K. Wang and Y. Shen, *Langmuir*, 2014, **30**, 6990-6998.

16 J.-H. Yang, Y. J. Gao, W. Zhang, P. Tang, J. Tan, A.-H. Lu and D. Ma, *J. Phys. Chem. C*, 2013, **117**, 3785-3788.

17 B. K. Erickson, R. Erni, Z. Lee, N. Alem, W. Gannett and A. Zettl, *Adv. Mater.*, 2010, **22**, 4467-4472.

18 B. G. Eda, Y.-Y. Lin, C. Mattevi, H. Yamaguchi, H.-A. Chen, I.-S. Chen, C.-W. Chen and M. Chhowalla, *Adv. Mater.*, 2010, **22**, 505-509.

19 Z. B. Liu, Y. Wang, X. L. Zhang, Y. F. Xu, Y. S. Chen, and J.G. Tian, *Appl. Phys. Lett.*, 2009, **94**, 021902.

20 Z.-B. Liu, X. Zhao, X.-L. Zhang, X.-Q. Yan, Y.-P. Wu, Y.-S. Chen and J.-G. Tian, *J. Phys. Chem. Lett.*, 2011, **2**, 1972-1977.

21 X.-F. Jiang, L. Polavarapu, S. T. Neo, T. Venkatesan and Q.-H. Xu, *J. Phys. Chem. Lett.*, 2012, **3**, 785-790.

22 W. N. Song, C. Y. He, W. Zhang, Y. C. Gao, Y. X. Yang, Y. Q. Wu, Z. M. Chen, X. C. Li and Y. L. Dong, *Carbon*, 2014, **77**, 1020-1030.

RSC Advances Accepted Manuscript

23 R. Yamuna, S. Ramakrishnan, K. Dhara, R. Devi, N. K Kothurkar, E. Kirubha and P. K. Palanisamy, *J. Nanopart. Res*., 2013, **15**, 1399.

24 M. B. Murali Krishna, N. Venkatramaiah, R. Venkatesanb and D. N. Rao, *J. Mater. Chem*., 2012, **22**, 3059-3068.

25 P.-P. Li, Y. Chen, J. H. Zhu, M. Feng, X. D. Zhuang, Y. Lin and H. B. Zhan, *Chem. Eur. J*, 2011, **17**, 780-785.

26 K. Sanusi and T. Nyokong, *J. Photoch. Photobio*. *A*, 2015, **303**, 44-52.

27 Y. Liu, S. M. O'Flaherty, Y. Chen, Y. Araki, J. R. Bai, J. Doyle, W. J. Blau and O. Ito, *Dyes and Pigments*, 2007, **75**, 88-92.

28 J. H. Zhu, Y. X. Li, Y. Chen, J. Wang, B. Zhang, J. J. Zhang and W. J. Blau, *Carbon*, 2011, **49**, 1900-1905.

29 J. Thompson, A. Crossley, P. D. Nellista and V. Nicolosi, *J. Mater. Chem.*, 2012, **22**, 23246-23253.

30 L. L. Tao, B. Zhou, G. X. Bai, Y. G. Wang, S. F. Yu, S. P. Lau, Y. H. Tsang, J. Q. Yao and D. G. Xu, *J. Phys. Chem. C*, 2013, **117**, 23108-23116.

31 X. Q. Zheng, M. Feng, Z. G. Li, Y. L. Song and H. B. Zhan, *J. Mater. Chem. C*, 2014, **2**, 4121-4125.

32 L. Jiang, F. S. Lu, H. M. Li, Q. Chang, Y. L. Li, H. B. Liu, S. Wang, Y. L. Song, G. L. Cui, N. Wang, X. R. He and D. B. Zhu, *J. Phys. Chem. B*, 2005, **109**, 6311-6315.

33 C. Y. He, J. Z. Fan, Z. G. Li, Y. C. Gao, Z. M. Chen, Y. L. Song, Y. Q. Wu and B. Wang, *Opt. Mater.*, 2014, **36**, 746-752.

34 N. Sheik-Bahae, A. A. Said, T. H. Wei, D. J. Hagan and E. W. Van Stryland, *IEEE J. Quantum. Elect*, 1990, **26**, 760-769.

35 C. Y. He, G. Shi, W. B. Duan, Y. Q. Wu, Z. M. Chen, W. N. Song, R. X. Zou and Y. L. Song, *J. Porphyrins Phthalocyanines*, 2009, **13**, 1243-1249.

36 V. Iliev, V. Alexiev and L. Bilyarska, *J. Mol. Catal. A-Chem*., 1999, **137**, 15-22.

37 T. Inoue, M. Moriguchi and T. Ogawa, *Thin Solid Films*, 1999, **350**, 238-244.

RSC Advances Accepted Manuscript

38 W. Gao, in *Springer Handbook of Nanomaterials*, ed. R. Vajtai, Springer, Berlin, 2013, ch. 15, pp. 571-603.

39 J. Locklin, K. Shinbo, K. Onishi, F. Kaneko, Z. Bao and R. C. Advincula., *Chem. Mater.*, 2003, **15**, 1404-1412

40 W. Dou, Q. Yang and C.-S. Lee, *J. Phys. Chem. C*, 2012, **116**, 19278-19284

41 A. Chunder, T. Pal, S. I. Khondaker and L. Zhai, *J. Phys. Chem. C*, 2010, **114**, 15129-15135

42 N. Liaros, P. Aloukos, A. Kolokithas-Ntoukas, A. Bakandritsos, T. Szabo, R. Zboril and S. Couris, *J. Phys. Chem. C*, 2013, **117**, 6842-6850

43 W. Wu, S. Zhang, Y. Li, J. Li, L. Liu, Y. Qin, Z.-X. Guo, L. Dai, C. Ye and D. Zhu, *Macromolecules*, 2003, **36**, 6286-6288

44 Y. Gao, X. Zhang, Y. Li, H. Liu, Y. Wang, Q. Chang, W. Jiao and Y. Song, *Opt. Commun.*, 2005, **251**, 429-433

RSC Advances Accepted Manuscript